Marine and Petroleum Geology 113 (2020) 104131

Contents lists available at ScienceDirect

Marine and Petroleum Geology

journal homepage: www.elsevier.com/locate/marpetgeo

Research paper

Insights from electron backscatter diffraction into the origin of fibrous calcite veins in organic-rich shale from lower Es3 to upper Es4, Jiyang Depression, China

Cunfei Ma[a,b,c,d,e,*], Chunmei Dong[a,b,c,d], Derek Elsworth[f], Qian Wang[g], Zhi Huang[h], Hailei Liu[g], Guoqiang Luan[a], Baojun Yu[i], Dan Li[j], He Yin[g], Meng Feng[k], Yueming He[a]

[a] School of Geosciences in China University of Petroleum (East China), Qingdao 266580, China
[b] Key Laboratory of Deep Oil & Gas Geology and Geophysics (China University of Petroleum), Ministry of Education, Qingdao 266580, China
[c] Reservoir Geology Key Laboratory of Shandong Province (East China), Qingdao 266580, China
[d] Research Laboratory of China University of Petroleum (East China), Key Laboratory of Oil and Gas Reservoir of China National Petroleum Corporation, Qingdao 266580, China
[e] Key Laboratory of Shale Oil and Gas Exploration & Production, SINOPEC, Dongying 257100, China
[f] The Pennsylvania State University (University Park), State College, PA 16803, USA
[g] Research Institute of Exploration and Development, Xinjiang Oilfield Company, PetroChina, Karamay 834000, China
[h] Tianjin Branch of Bohai Sea Oil Field Research Institute, CNOOC, Tianjin 300459, China
[i] Brucker Company, Shanghai 200000, China
[j] School of Earth Science and Engineering in Hebei University of Engineering, Handan 056038, China
[k] Xibu Drilling Engineering Company Limited, CNPC, Karamay 834000, China

ARTICLE INFO

Keywords:
Fibrous calcite veins
Electron backscatter diffraction
Crystal habit
Growth direction
Growth temperature
Stress condition

ABSTRACT

The origin of fibrous calcite veins developed in organic-rich shales, has attracted great attentions. However the growth direction, formation temperature and stress state are still controversial. The calcite veins in organic-rich shale from lower Es3 to upper Es4 in the Jiyang Depression has been analyzed with electron backscatter diffraction technology (EBSD), which can characterize the microstructures and orientation of mineral crystals in situ. On the basis of core observation and microscopic identification of petrological characteristics, the longitudinal and horizontal profiles of calcite veins were measured by EBSD. Crystallographic information on calcite veins, obtained by pattern quality mapping, phase diagrams, grain distribution maps, Euler graphs, grain misorientations and pole figures, clarifies the origins of these veins. The results show that calcite crystals in calcite veins belong to the sharp-rhombohedral space lattice structure of the trigonal system. Calcite crystals have a preferred orientation on the longitudinal profile, while there is no obvious preferred orientation on the horizontal profile. On the longitudinal profile of calcite veins, the misorientation of calcite crystals is the cause of the interference colour and extinction difference of calcite crystals under orthogonal light. The crystal interference and extinction characteristics on both sides of middle line in calcite veins are different, indicating that the growth direction of calcite veins is syntaxial. A shallow burial environment is suggested for calcite veins initial forming by the evidence that crystal morphology of calcite in calcite veins is most in the shape of sharp-rhombohedron, and some of which have hexagonal prism shape. The average orientation difference of calcite veins on longitudinal and horizontal profiles indicates that the average orientation of calcite grains is inhomogeneous. The stress concentration of small grains is higher than that of large grains, and cracks are developed in the interior or on the border of calcite grains on the longitudinal profile, which indicates that calcite veins are formed in the stress environment of three directional extrusion circumstances.

1. Introduction

Fibrous calcite veins are widely developed in organic-rich shales, and such veins that infill bedding cracks are often referred to as “beef” or “cone-in-cone” (Cobbold et al., 2013). Research on fibrous calcite veins has mainly focused on aspects such as petrological

* Corresponding author. School of Geosciences in China University of Petroleum (East China), Qingdao 266580, China.
E-mail address: mcf-625@163.com (C. Ma).

https://doi.org/10.1016/j.marpetgeo.2019.104131
Received 7 September 2019; Received in revised form 6 November 2019; Accepted 8 November 2019
Available online 13 November 2019
0264-8172/

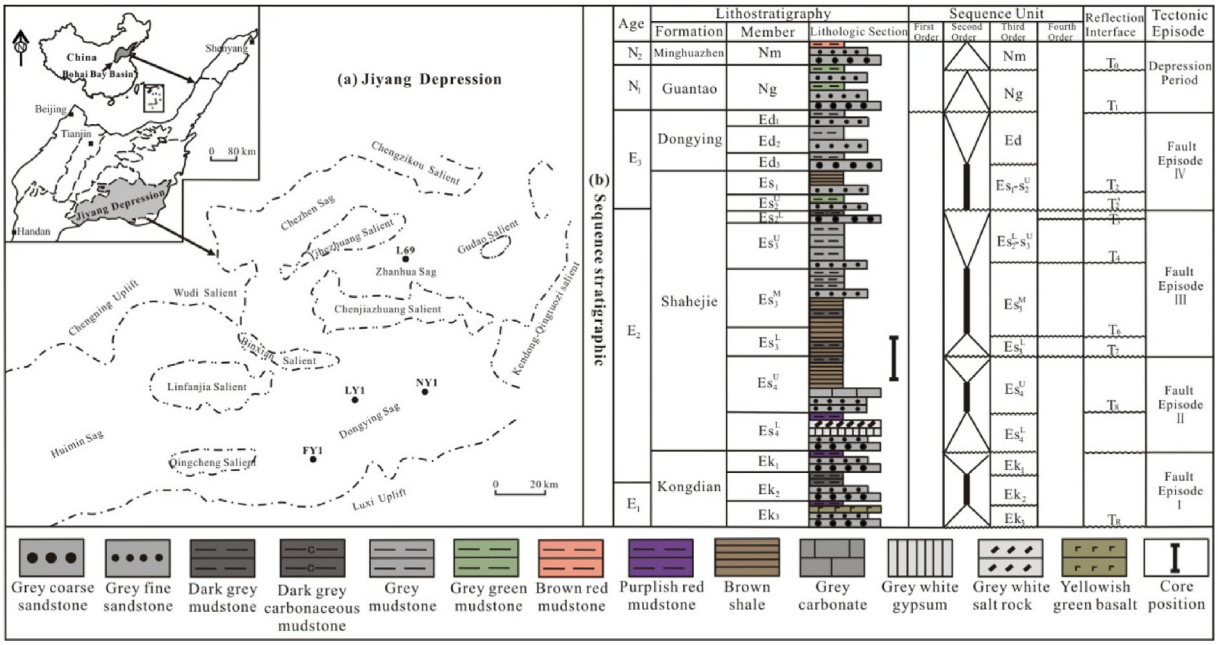

Fig. 1. Geography and sequence stratigraphic map of research area.

characterization, formation of bedding cracks and veins (Gale et al., 2007; Ramsay, 1980; Wang et al., 2018). The formation of bedding cracks is the key to reveal the origin of fibrous calcite veins, but the stress conditions for the formation of cracks are controversial (Cobbold and Rodrigues, 2007; Cobbold et al., 2013; Gale et al., 2014; Li et al., 2013; Luo et al., 2015; Ma et al., 2016). Research on the origin of fibrous calcite veins has included the source and migration of veins (Bons and Jessell, 1997; Putnis et al., 1995; Taber, 1918), vein growth direction (Bons and Montenari, 1997), genesis mechanism of veins (Meng et al., 2017; Shovkun and Espinoza, 2018; Ukar et al., 2017), formation time of veins and the evolution model of veins (Wang et al., 2005; Zhang et al., 2016). There is controversy about the direction of vein growth, which can be divided into antitaxial, syntaxial and tensile types (Bons and Montenari, 2005). Calcite veins are generally believed to be formed in the oil-generating stage of source rocks (Wang et al., 2005; Zhang et al., 2016), however, it is difficult to find evidence of fluid inclusions in calcite veins (Cobbold et al., 2013), and synsedimentary deformation characteristics found in some calcite veins also indicate that the veins were formed in the early diagenetic stage. It is generally believed that the veins are formed by calcite crystals filling cracks (Maher et al., 2017; Meng et al., 2017; Ukar et al., 2017) and the crystallization dynamics of fibrous minerals is an important factor in changing the local stress state of rocks (Shovkun and Espinoza, 2018; Taber, 1916, 1918). Therefore, the growth conditions of calcite veins are difficult to determine.

Improved mineral analysis and testing technologies, such as multi-purpose thin section, field emission scanning electron microscope (FESEM) and electron backscatter diffraction (EBSD), have been applied to the study of fibrous calcite veins. Among them, core - thin section - FESEM achieves multi-scale characterization of calcite veins (Gale et al., 2007; Loucks et al., 2012; Milliken and Day-Stirrat, 2013). In particular, EBSD technology has been increasingly applied in the study of phase identification, crystal orientation and micro-stress-strain information of calcite veins (Ming et al., 2016; Villert et al., 2009; Zhang et al., 2015), and this provides an entry point and powerful means for studying the mechanical coupling mechanism of bedding cracks and fibrous calcite veins (Huang and Pan, 2010; Maurice et al., 2013; Wilkinson et al., 2009). EBSD has been widely used in industrial fields, especially in material research (Yang, 2008). Its typical applications include grain size, macro-texture, micro-texture, recrystallization, strain analysis (Keshavarz and Barnett, 2006), grain boundary characterization, CSL grain boundary, phase identification, phase distribution and phase transition process and failure analysis (Azpiroz et al., 2007; Nowell and Wright, 2005). In the field of geosciences, EBSD technology has also been rapidly applied, including mineral phase identification, crystal orientation and growth direction analysis, twin law and structure analysis (Liu et al., 2008; Prior et al., 1999; Zaefferer and Wright, 2007). At present, EBSD technology is widely used in the field of tectonic geology to study the micro-structural characteristics of rocks and minerals and reveal the deformation mechanism (Heidelbach et al., 2000; Lloyd, 2000; Mainprice et al., 2004; Toy et al., 2008; Xu et al., 2009). In this paper, the crystallographic information reflecting growth conditions of calcite crystals in the fibrous calcite veins developing in organic-rich shale is obtained by EBSD, and then the origin of the fibrous calcite vein can be inferred, which is of theoretical significance to reveal the structural diagenesis mechanism of fibrous calcite veins, and has certain application value to guide the shale oil and gas exploration.

2. Overview of the research area

The shale samples were collected in the Jiyang Depression, which is part of the primary tectonic unit of the Bohai Bay Basin in East China, and is located west of the Tan-lu fault zone, south of the Chengning uplift and the north of the Luxi uplift. The Jiyang Depression is a Mesozoic–Cenozoic rift–depression composite basin composed of four negative secondary tectonic units including Dongying, Huimin, Zhanhua, and Chezhen Sags, along with several positive secondary tectonic units including the Gudao, Yihezhuang, Chenjiazhuang, Wudi, Binxian, and Kendong Qingtuozi highs. Dongying and Zhanhua Sags are the richest hydrocarbon accumulation areas in the Jiyang Depression, and all have significant oil production. FY1, LY1, NY1 and L69 are four key shale oil wells of lower Es3 to upper Es4 in the Paleocene Shahejie Formation (Fig. 1a).

The Shahejie Formation was formed in a lacustrine transgression systems tract (LTST) or a lacustrine highstand systems tract (LHST) of second-order sequence (Fig. 1b). Owing to continuous subsidence, terrigenous detritus was injected in deposits of the thick lacustrine formation with a vast biodiversity. Especially during the fault depression stage, thick, dark strata of brown shale and dark grey mudstone

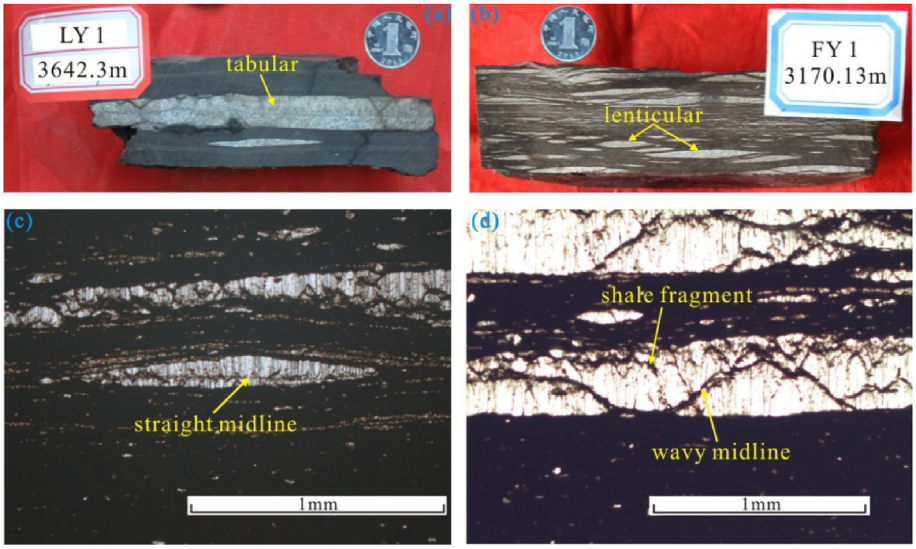

Fig. 2. Characteristics of calcite veins. (a) The calcite vein develops in tabular shape; (b) Calcite veins develop in lenticular shape; (c) The calcite vein develops straight midline; (d) The calcite vein develops wavy midline and is filled with shale fragments among calcite crystals.

developed under deep water depths, with brackish, or saline water under alkaline and reducing conditions of lower Es3 to upper Es4 of Shahejie Formation (Fig. 1b).

3. Sample preparation

Calcite veins mainly develop in organic-rich shales of lower Es3 to upper Es4 in the study area. The calcite veins are several millimeters to tens of centimeters long and several microns to several centimeters wide on the longitudinal profile. They are mainly of tabular or lenticular shapes (Fig. 2a and b). There is usually a dark intermediate line in calcite veins, which is mainly composed of mud and this line can be straight or wavy (Fig. 2c and d). Calcite crystals on both sides of the intermediate line are arranged symmetrically, and the shale fragments are captured among calcite crystals.

Two pieces of the same calcite vein were taken out with a knife for the longitudinal and horizontal profile tests. Then, the taken out samples were polished with abrasive papers of 400, 800, 1500, 2000 and 2500 successively. After that, Leica EM TXP mechanical profiler was used to finish the mechanical polishing of calcite veins, and then Gatan 697 Ilion II argon ion profiler was used for further sectioning. After argon ion polishing, the strain layer on the surface of calcite veins resulting from sample preparation was removed. Finally, a 10-nm thick carbon film was deposited on the surface of calcite veins by carbon plating instrument and the backscatter probe of FESEM was used to test the charge effect.

4. Principle of electron backscatter diffraction technique test

The longitudinal and horizontal profiles of the same calcite vein were scanned and tested respectively according to the flow chart of electron backscatter diffraction and data acquisition in Figs. 3 and 4 (Michael et al., 2003). The EBSD test was carried out on an electron backscatter diffraction device (Quantax EBSD 400i) mounted on an environmental scanning electron microscope (Quattro S). The working conditions are acceleration voltage 20 kV, beam current 6 nA, sample tilt angle 70° and working distance 25 mm.

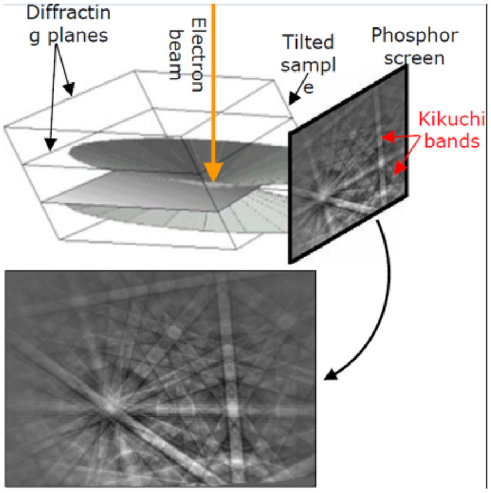

Fig. 3. Schematic diagram of electron backscatter diffraction test.

5. Results

5.1. Pattern quality map

The Pattern Quality Map characterizes the quality of the Kikuchi pattern. The higher the brightness, the better the quality of the Kikuchi pattern. The pattern quality map of the longitudinal profile of calcite veins clearly shows the longitudinal extension of calcite crystals (Fig. 5a), while the pattern quality map of the horizontal profile shows that calcite crystals are allotriomorphic granular (Fig. 5b). At the same time, the pattern quality chart also indicates that the calcite veins are in good condition.

5.2. Phase diagram

The energy spectrum probe, which is combined with the electron backscatter diffraction probe (EBSD) on scanning electron microscope, can be used to make the rapid phase identification of calcite veins on both longitudinal and horizontal profiles. Energy spectrum scanning results show that the identified phase of calcite reaches 94.5% of the total veins. The unrecognized phase accounts for 5.5%, which usually belongs to non-crystal, non-calcite bodies captured during the growth

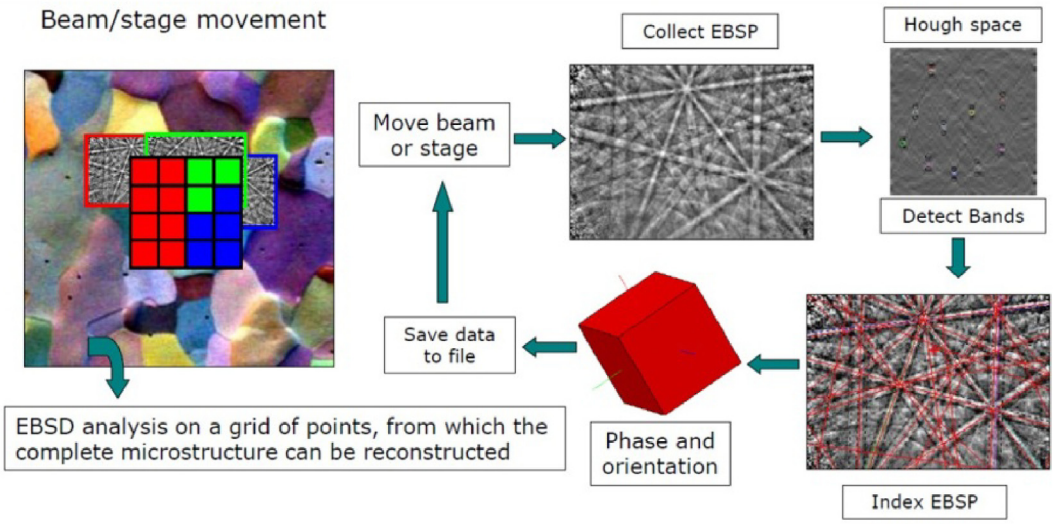

Fig. 4. Automatic data collection process of electron backscatter diffraction.

of calcite crystals, such as shale fragments, argillaceous or organic matter (Fig. 6).

5.3. Grain distribution map

The grain distribution map is used to describe the shape, size and grain boundary of the grains in the area analyzed, including the number of grains, average grain size, average grain size of each phase, the distribution of the ratio of the length of the long axis to the short axis, and the concentration of the long axis direction of the grains. Because the calcite veins extend columnarly on the longitudinal profiles and are of allotriomorphic granular shapes on the horizontal profiles, the grain size cannot be measured easily on the longitudinal profiles. Therefore, the crystal size was measured on the horizontal profiles. The statistical results show that the average grain size of calcite on the horizontal profiles is 17.6 μm (Fig. 7).

5.4. Euler graph

Two coordinate systems are involved in the process of EBSD testing and processing. One is the sample coordinate system indicating the spatial position of the sample. Usually, the surface of the sample is the X- and Y-axis, the direction perpendicular to the surface of the sample is Z-axis (Fig. 8a). The other coordinate system is the crystal coordinate system used for crystal orientation. The four-axis orientation method (hkil) is usually used in the trigonal system and the hexagonal system, and the three-axis orientation method is adopted in other systems (Fig. 8a). The Euler graph, the distribution of the Euler angle index, is usually expressed by ($\phi1$, Φ, $\phi2$), which is used to represent the spatial arrangement of crystal coordinates relative to sample coordinates. The Euler graph lays a theoretical foundation for the study of crystal orientation. There is a crystal coordinate for each crystal of the calcite vein. The position of the crystal in the sample coordinate system can be obtained after three rotations according to the Euler angle (Fig. 8b). Owing to the certain growth law of the same grain, the spatial orientation of the crystals formed in the grain is the same, and the Euler angle indexes of grains are the same. Therefore, on the Euler graph of the longitudinal profile of calcite veins, the same Euler angle index exists in the same grain extending longitudinally, indicating the same crystal orientation (Fig. 9a). However, on the Euler graph of the horizontal profile, the same Euler angle index can exist both in the same grain and in different grains. It indicates that the same grain and different grains can both have the same crystal orientation (Fig. 9b). Sharp-rhombohedral cells are shown by the calculated crystal cell

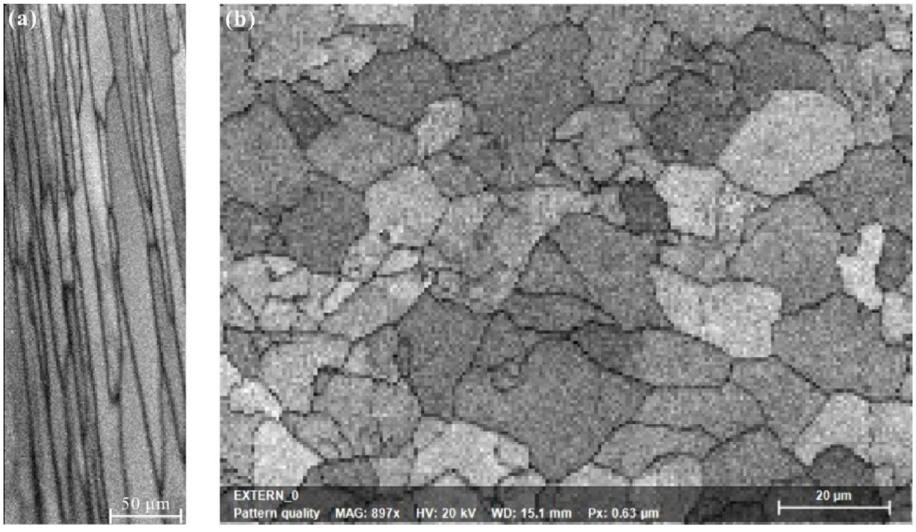

Fig. 5. Pattern quality map of calcite veins. (a) Longitudinal profile; (b) horizontal profile.

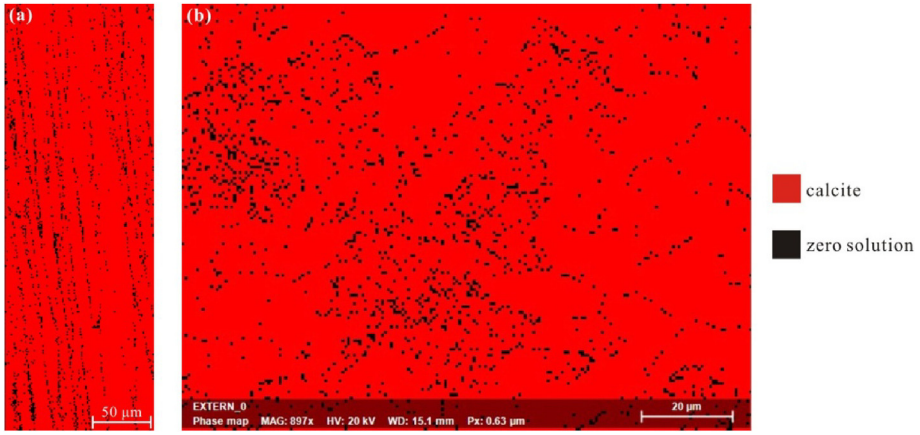

Fig. 6. Phase identification of calcite veins. (a) Longitudinal profile; (b) horizontal profile.

parameters (Fig. 9c and d).

5.5. Grain mis-orientation

The Euler graph solves the issue of converting any crystal from the crystal coordinate system to the sample coordinate system, or vice versa, and determines the orientation of the crystal. Therefore, the orientation difference between any two points can be further determined by statistics, and the orientation difference distribution of all crystals can be obtained.

It is shown in Fig. 10a that two points on the longitudinal profile of calcite veins are located on two adjacent crystals. One of the crystals has an orientation close to 0°, while the other has an orientation close to 80° (Fig. 10b). The orientation difference between the two crystals is about 70°. According to the above statistical method of two points, the misorientation of crystals on the whole longitudinal profile is between 0° and 100° (Fig. 10c). There are two dominant misorientations, 12° and 63° (Fig. 10c). It is indicated that there are two dominant growth directions of the crystals in the calcite vein on the longitudinal profile, one of which has 12° misorientation and the other has 63° misorientation.

It is shown in Fig. 11a that two points on the horizontal profile of calcite veins are located on two adjacent crystals. One of the crystals has an orientation close to 0°, while the other has an orientation close to 55° (Fig. 11b). The grain misorientation between the two crystals is about 55°. Similarly, according to the above statistical method of two points, the misorientation of crystals on the whole horizontal profile is between 0° and 100° (Fig. 11c). The crystal orientation of calcite veins is not obvious on the horizontal profile, but there is one dominant misorientation, which is 64° (Fig. 11c). It implies that the orientations of the crystal of calcite veins on the horizontal profile are complex, with a dominant relative superior growth direction. The misorientation is 64°.

5.6. Pole figure

After projecting the intersection of a normal line and a projected sphere of each grain in a polycrystalline sample placed at the center of a projected sphere onto the equatorial plane representing the macroscopic direction of the sample, the points with the same pole density can be connected to form isodensity lines, and this finally forms a pole figure which can show the distribution of texture. Since only the poles of a particular crystal plane are projected on this map, other crystal planes are not projected, so this pole figure is the one of that particular crystal plane. The pole figure can reflect the preferred orientation in the sample, which is generally expressed by the pole figure of the crystal plane with low index.

On the longitudinal profile of calcite veins, the poles are concentrically distributed in two positions (Fig. 12a) on the polar map of crystal plane (0001), which indicates that the growth orientation of crystal planes (0001) in calcite veins is relatively stable, and there are two dominant orientations. On the polar graphs of crystal planes ($2\bar{1}\bar{1}0$)

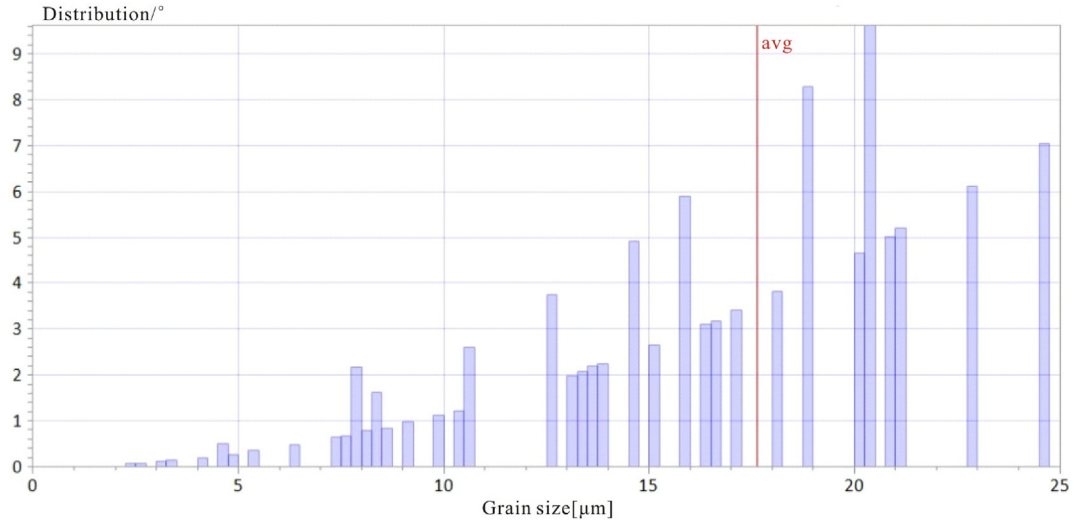

Fig. 7. Statistics of grain size on the horizontal profiles of calcite veins.

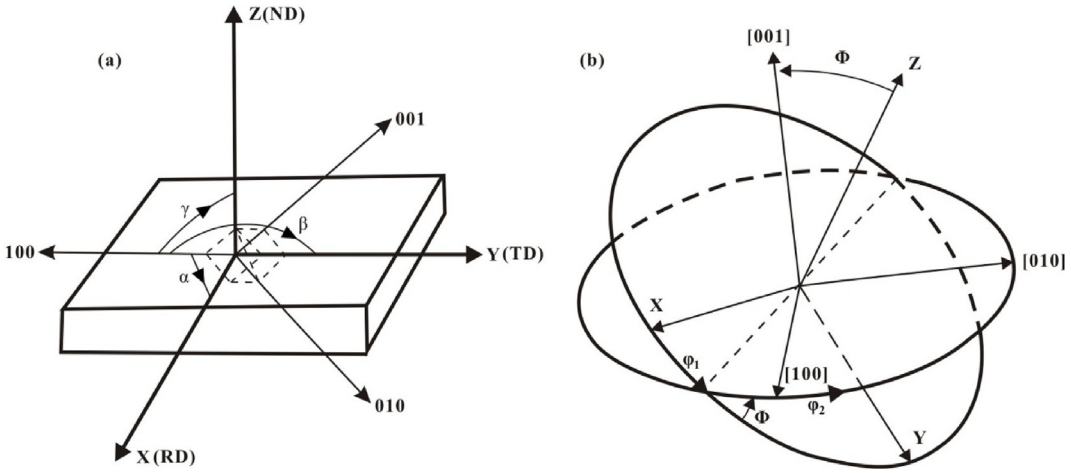

Fig. 8. Schematic diagram of sample coordinate system, crystal coordinate system and Euler angle indicating crystal orientation.

and crystal planes $(01\bar{1}0)$, the poles are intersected by two bands (Fig. 12b and c), indicating that the crystal planes $(2\bar{1}\,\bar{1}0)$ of the crystals in calcite veins are nearly parallel, forming two crystal bands, and the same is true of the crystal planes $(01\bar{1}0)$.

On the horizontal profile of calcite veins, the poles are distributed dispersedly on the polar graph of crystal plane (0001), which indicates that the growth directions of crystals on the horizontal profile of calcite veins are various and the preferred orientation is not obvious (Fig. 13a). However, on the pole figures $(2\bar{1}\,\bar{1}0)$ and $(01\bar{1}0)$, it can be seen that some poles form triangular bands (Fig. 13b) and rhombic bands (Fig. 13c), with an acute angle of about 60°.

6. Discussion

6.1. Crystal habit

On the longitudinal profile of calcite veins, the misorientation of one group of crystals is 12°, which is close to parallel, while that of the other group is 63°, which is close to 60°. On the horizontal profile, the misorientation of a group of crystals is 64°, which is also close to 60°. The crystal orientation on the longitudinal and horizontal profiles in calcite veins conforms to the sharp-rhombohedral space lattice structure of trigonal system, that is, the profile parallel to the symmetrical axis of the apical rhombohedral body is quadrilateral, while the profile perpendicular to the symmetrical axis of the apical rhombohedral body

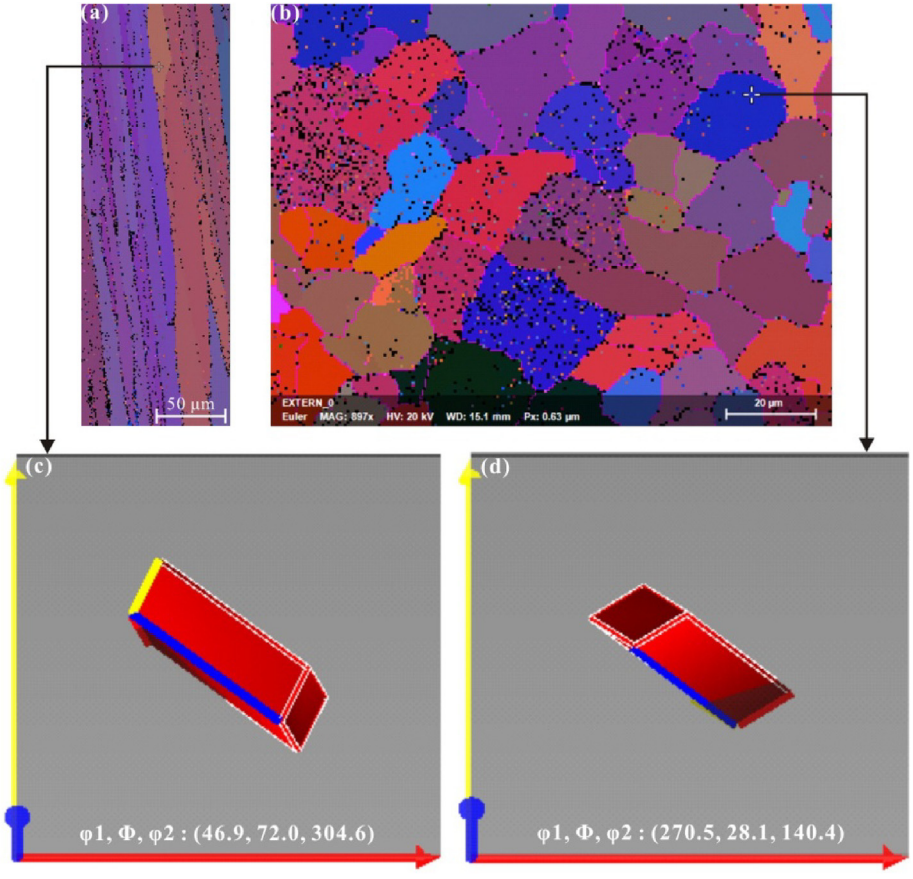

Fig. 9. Euler graph and orientation figure of crystals of calcite veins. (a) Euler graph of the crystal on the longitudinal profile; (b) Euler graph of the crystal on the horizontal profile; (c) Crystal forms and orientation at a certain location on the longitudinal profile of calcite veins; (d) Crystal forms and orientation at a certain location on the horizontal profile of calcite veins.

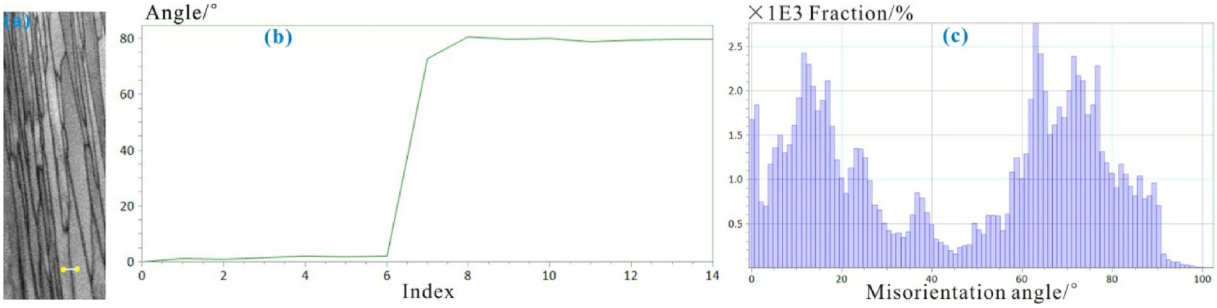

Fig. 10. The grain misorientation of calcite crystals on the longitudinal profile. (a) Two positions on the longitudinal profile; (b) The grain misorientation between the two crystals on the longitudinal profile; (c) The grain misorientation distribution on the longitudinal profile.

is triangular. The macro-extension structure of veins is constrained by the microcosmic growth law of crystals.

In addition, consistent with the conclusion of the misorientation on the longitudinal profile of calcite veins, the crystal plane (0001), $(2\bar{1}\bar{1}0)$ and $(01\bar{1}0)$ of crystals on the longitudinal profile of calcite veins is concentrically distributed or forms two intersecting crystal zones, which indicates that calcite veins have a preferred orientation on the longitudinal profile. In addition, the poles in the crystal plane (0001) pole figure of calcite veins are scattered, while the poles in the crystal plane $(2\bar{1}\bar{1}0)$ and $(01\bar{1}0)$ pole figure generally form triangular or rhombic crystal bands. The above observation results show that calcite veins do not have obvious preferential orientation on the horizontal profile, but generally have the development trend of triangular or rhombic orientation. Therefore, the crystal growth in calcite veins conforms to the characteristics of the triangular system, where the crystal always extends along the high-grade crystal axis and shows a symmetrical distribution in other directions. The macro-orientation characteristics on the longitudinal and horizontal profiles of calcite veins are constrained by the micro-growth law of the triangular system crystals.

Since the calcite crystals in the calcite veins are of sharp-rhombohedral shape and extend longitudinally, it can be inferred that the calcite veins are mainly composed of sharp-rhombohedral calcite crystals superimposed vertically along the symmetrical axis in the study area (Fig. 5a). Since the trigonal and hexagonal systems can usually be converted to each other and the three rhombohedrons can form a hexagonal prism, the horizontal profile of calcite veins is allotriomorphic granular. In fact, the ideal complete form is hexagonal, rhombic or triangular. However, limited by the underground crystallization conditions such as crystallization speed and space, the development of hexagon, rhombus and triangle is incomplete, and the boundary is concave or convex, showing allotriomorphic granular (Fig. 5b).

6.2. Growth direction

The sharp-rhombohedral l crystals in calcite veins extend columnarly along the optical axis, and the calcite crystals are optic uniaxial crystal (−) (Ne < No) (Fig. 14a). On the longitudinal profile of calcite veins, the direction is close to the orientation of Ne and No axes of the optical indicatrix, which have the largest birefringence and the largest optical path difference. Thus, the maximum interference colour under orthogonal light is generated, which is called advanced white interference colour (Fig. 14b). Due to the misorientation between adjacent grains on the longitudinal profile of calcite veins, the birefringence index of the grains cut on the longitudinal profile is different, which results in the impurity of the advanced white interference colour, and gives rise to a band of variegated tones composed of blue, green, yellow, orange, red and violet. In addition, the misorientation between grains results in the difference in the orientation of the optical indicatrix, which further leads to the difference in the orientation of the Ne and No axes of the optical indicatrix cut. Thus, the polarization direction of light in some grains parallel to the Ne axis or the No axis produces complete extinction (Fig. 14b), while some grains have interference colour. However, the orientation difference between the grains growing in the same direction does not vary much and usually has the same extinction characteristics. In the horizontal plane of calcite veins, the main cut is to, or near to, the Ne and No axes of the optical indicatrix of calcite crystals, and the birefractive index is zero or nearly zero, resulting in the minimum optical path difference. Therefore, under the orthogonal light, it appears as complete extinction or first greyish white interference colour (Fig. 14c).

Most calcite veins containing middle lines, and calcite crystals on both sides of a given point on the middle line showing generally the same interference and extinction characteristics with some dislocations (Fig. 15a), indicated that there are some differences in orientation between the two sides of calcite veins in the process of crystal growth. All the evidence discussed above suggested that calcite crystals initiated from both outsides towards the middle line (inner side). The calcite veins that are recrystallizing and the remnants of early heteromorphic granular calcite crystals can be seen in Fig. 15b. Therefore, the misorientation of calcite crystals observed by EBSD is the reason for the difference in interference colour and extinction of calcite crystals under orthogonal light. The difference in crystal interference and extinction characteristics between the two sides of the middle line of calcite veins at the same position indicates that the growth direction of calcite veins

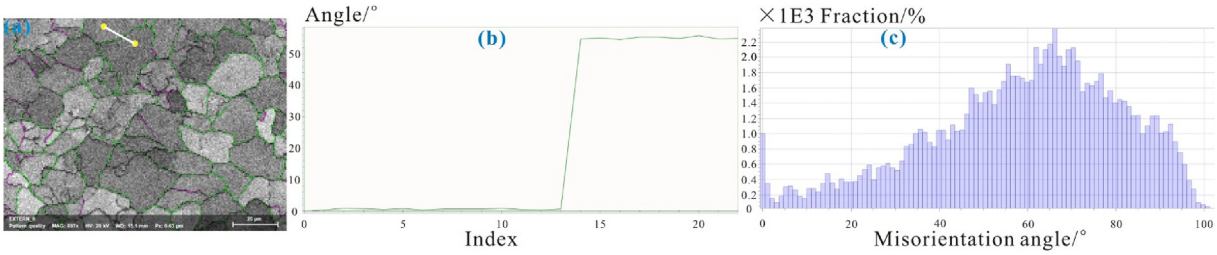

Fig. 11. The grain misorientation of calcite crystals on the horizontal profile. (a) Two positions on the horizontal profile; (b) The grain misorientation between the two crystals on the horizontal profile; (c) The grain misorientation distribution on the horizontal profile.

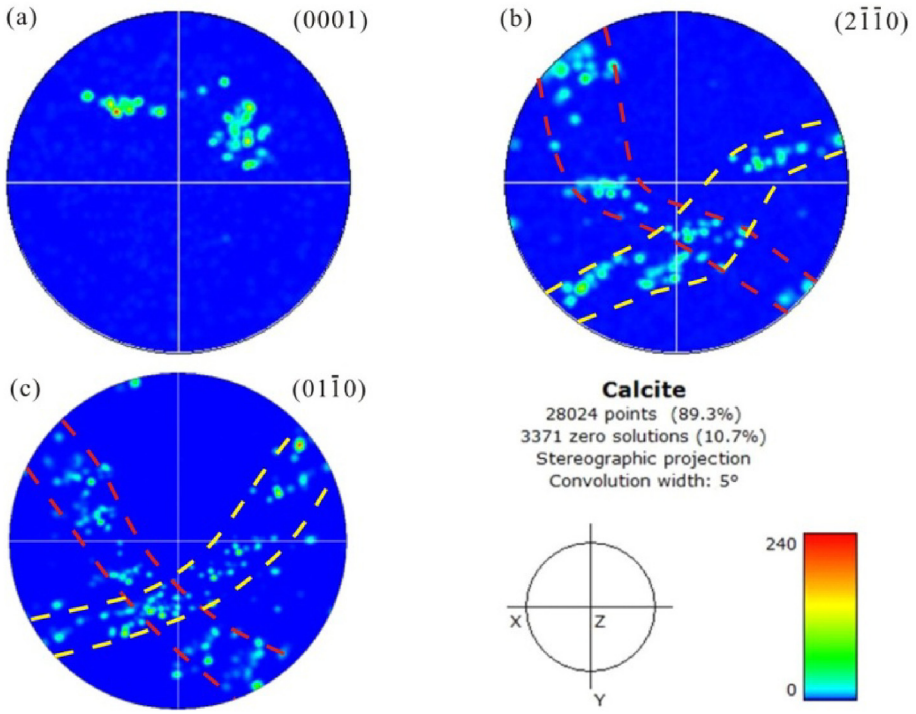

Fig. 12. Crystal pole figures of calcite crystals on the longitudinal profile.

is from both sides to the middle. It belongs to the symmetric syntaxial growth direction (Bons and Montenari, 2005).

6.3. Growth temperature

Crystal morphology, structure and chemical composition can reflect the chemical composition of the diagenetic fluid, medium temperature and pressure, pH value, water-rock volume ratio, solid-liquid or liquid-liquid interface surface characteristics (Jones and Renaut, 1996; Qian et al., 2009). Morphology is controlled by the temperature and pH value of fluids, especially temperature. Hence, information about crystal structure and growth environment can be obtained by observing the crystal morphology (Wang, 1983). Calcite has various crystal forms, which are closely related to its growth temperature. With the decrease in growth temperature, the crystal shape tends to evolve from clinthetiform and obtuse rhombohedron to ditrigonal scalenohedron,

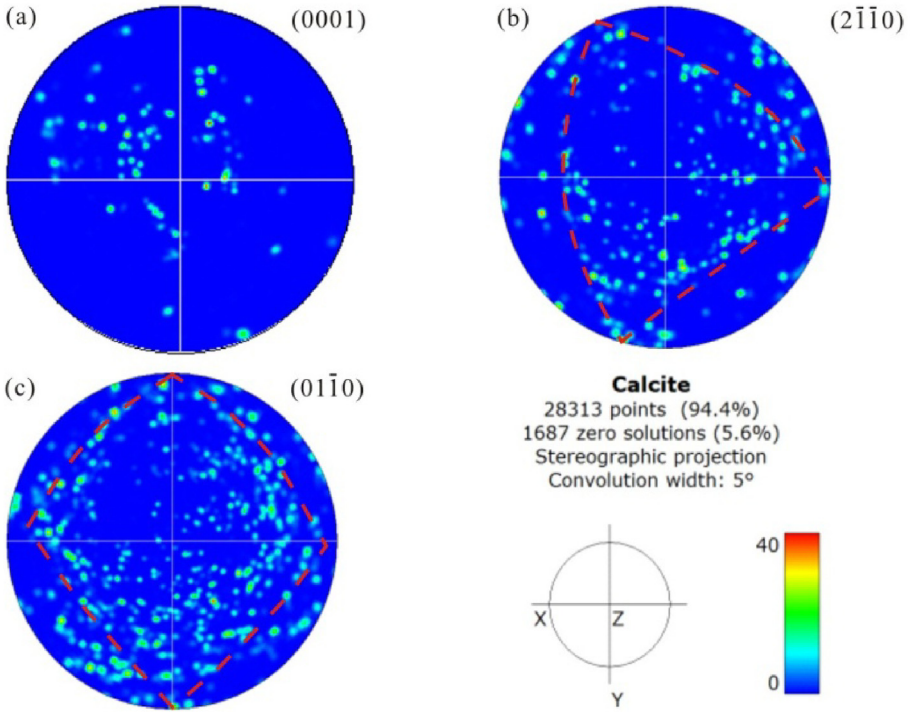

Fig. 13. Crystal pole figures of calcite crystals on the horizontal profile.

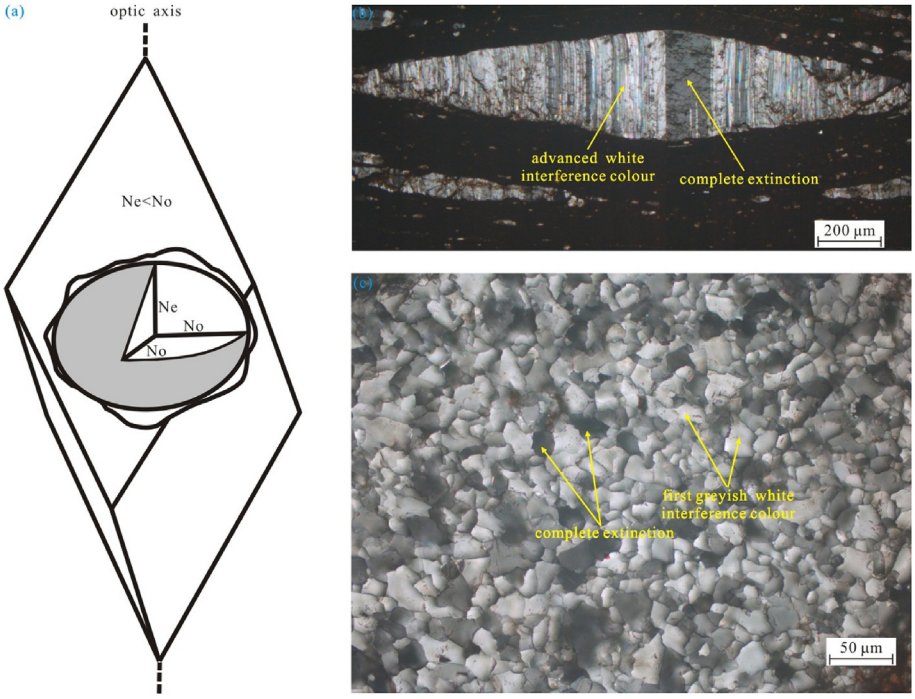

Fig. 14. The optical indicatrix and orthogonal light characteristics of calcite crystals in the calcite veins. (a) Sharp-rhombohedral calcite crystal and the optical indicatrix characteristics; (b) orthogonal light characteristics of calcite crystals on the longitudinal profile, with the characteristics of advanced white interference colour and complete extinction; (c) orthogonal light characteristics of calcite crystals on the horizontal profile, with the characteristics of first greyish white interference colour. (For interpretation of the references to colour in this figure legend, the reader is referred to the Web version of this article.)

hexagonal prism and sharp rhombohedron. According to M. H. Shkabara's research, the growth temperature of calcite with (0001) and (10$\bar{1}$1) form is 250–350 °C, the growth temperatures of calcite with (10$\bar{1}$0) and (01$\bar{1}$2) combination form is 150–250 °C, while the growth temperature of calcite with sharp-rhombohedral shape is 25–75 °C (Li, 1994). In addition, it is generally believed that hexagonal prism crystals occur at low temperature of crystallization environment. The crystal morphology of calcite veins in the study area is sharp-rhombohedral and some of them have hexagonal prism morphology, indicating that the initial growth temperature of calcite veins is low, which coincides with the late stage of organic matter biochemical gas generation and the early stage of thermal catalytic hydrocarbon generation, at a temperature of about 75 °C (Luan et al., 2019).

6.4. Stress condition

Calcite veins are usually of lenticular shape and fill in cracks. It is usually considered that cracks form under tension-shear stress, so calcite veins should develop under tension-shear stress. However, the average misorientation of the grains obtained by this EBSD test indicates that the calcite veins develop under the condition of three-dimensional compressive stress. Average grain misorientation is used to describe the difference between the orientation value of a crystal in the grain and the average orientation value of all crystals in the grain. It represents the change in crystal orientation in grains and reflects the degree of stress concentration. The average grain misorientation on the longitudinal and horizontal profiles of calcite veins is uneven within and between grains, and the stress concentration of small grains is higher than that of large grains (Fig. 16a and b). These results show that the crystals in calcite veins grow in competition in a limited space. The growth rate of large grains is fast, and they occupy the main space preferentially. The small grains can only grow in the space between large grains by extrusion, resulting in the stress concentration of small grains during extrusion (Fig. 16a and b). Hence, the extrusion of small grains can also occur during the growth of large grains. Ultimately, the calcite veins are not fully developed on the horizontal profile, showing allotriomorphic granularity (Figs. 5b and 16b). In addition, although the overall orientation of grains extending in the same direction on the longitudinal profile is roughly the same, the average misorientation of grains is different. This suggests that in the vertical extrusion environment, the early grains and the late grains interact during the growth process, resulting in the stress concentration of some grains. This results in a series of cracks in the grain interior or grain boundary (Fig. 16c).

7. Conclusion

The pattern quality map, phase diagram, grain distribution map, Euler graph, grain misorientation and pole figure of calcite veins obtained by electron backscatter diffraction (EBSD) technology can better

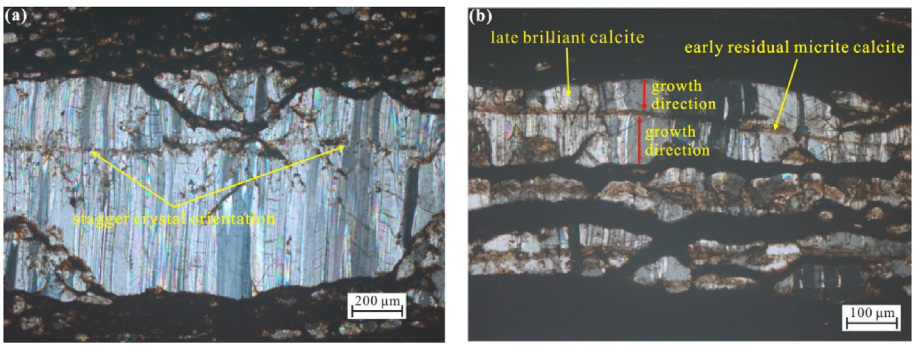

Fig. 15. The interference characteristics under orthogonal light and growth direction of calcite crystals of calcite veins. (a) The stagger of calcite crystals on different sides of the intermediate line in calcite veins results in crystal misorientation, which produces heterogeneity in the interference colour and extinction characteristics; (b) The early micrite calcite is recrystallizing into late sparry calcite from boundary to intermediate. (For interpretation of the references to colour in this figure legend, the reader is referred to the Web version of this article.)

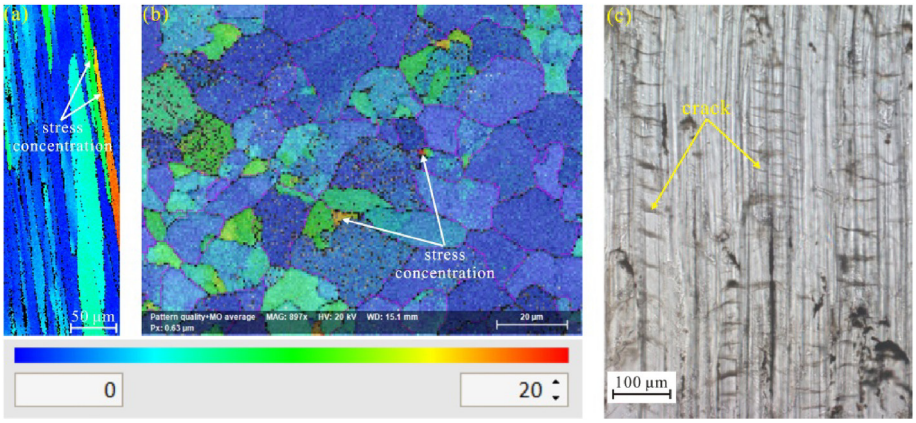

Fig. 16. Stress concentration and crack development of calcite veins. (a) The average misorientation of grains is different on the longitudinal profile, indicating that the small grains are in the extrusion stress state; (b) Cracks in the interior or boundary of the grain on the longitudinal profile of calcite veins.

characterize the crystal habit, growth direction, growth temperature and stress conditions during formation of calcite veins. Calcite crystals in calcite veins belong to the sharp-rhombohedral space lattice structure of trigonal system. The growth direction of calcite crystals belongs to symmetric syntaxial growth direction from the boundary to the middle of the veins. The initial growth temperature of the calcite crystals is low, and the calcite crystals are formed under the condition of three-dimensional compressive stress. The origin of fibrous calcite veins in organic rich shale is closely related to the bedding fracture and calcite crystal growth. EBSD technology provides a powerful solution to study the genetic mechanism and evolution of fibrous calcite veins, as well as reveal the coupling mechanism of structural diagenesis. The fibrous calcite vein not only provides reservoir space for shale reservoir, but also increases shale brittleness. Therefore, EBSD technology can be used to study the origin of the fibrous calcite vein for understanding the process of shale oil and gas migration and accumulation, as well as evaluating the fracturing effect of shale reservoir.

Acknowledgements

This work was supported by the Natural Science Foundation of China (Grant No. 41802172; 41830431), National Science Technology Major Project of China (Grant No. 2017ZX05009-001), Natural Science Foundation of Shandong Province of China (Grant No. ZR2018BD014), Natural Science Foundation of Hebei Province of China (Grant No. D2017402165), and Scientific and Technological Research Projects in Universities of Hebei Province of China (Grant No. QN2017036).

Appendix A. Supplementary data

Supplementary data to this article can be found online at https://doi.org/10.1016/j.marpetgeo.2019.104131.

References

Azpiroz, M., Lloy, G., Fernandez, C., 2007. Development of lattice preferred orientation in clinoamphiboles deformed under low-pressure metamorphic conditions: a SEM/EBSD study of metabasites from the Aracena metamorphic belt (SW Spain). J. Struct. Geol. 29 (4), 629–645.

Bons, P., Jessell, M., 1997. Experimental simulation of the formation fibrous veins by localised dissolution-precipitation creep. Mineral. Mag. 61 (1), 53–63.

Bons, P., Montenari, M., 2005. The formation of antitaxial calcite veins with well-developed fibres, Oppaminda Creek, South Australia. J. Struct. Geol. 27 (2), 231–248.

Cobbold, P., Rodrigues, N., 2007. Seepage forces, important factors in the formation of horizontal hydraulic fractures and bedding-parallel fibrous veins ('beef' and 'cone-in-cone'). Geofluids 7 (3), 313–322.

Cobbold, P., Zanella, A., Rodrigues, N., Helge, L., 2013. Bedding-parallel fibrous veins (beef and cone-in-cone): worldwide occurrence and possible significance in terms of fluid overpressure, hydrocarbon generation and mineralization. Mar. Pet. Geol. 43, 1–20.

Gale, J., Reed, R., Holder, J., 2007. Natural fractures in the Barnett Shale and their importance for hydraulic fracture treatments. AAPG (Am. Assoc. Pet. Geol.) Bull. 91 (4), 603–622.

Gale, J., Laubach, S., Olson, J., Peter, E., András, F., 2014. Natural fractures in shale: a review and new observations. AAPG (Am. Assoc. Pet. Geol.) Bull. 98 (11), 2165–2216.

Heidelbach, F., Kunze, K., Wenk, H., 2000. Texture analysis of a recrystallized quartzite using electron diffraction in the scanning electron microscope. J. Struct. Geol. 22 (1), 91–104.

Huang, Y., Pan, C., 2010. Micro-stress-strain analysis in materials based upon EBSD technique: a review. J. Chin. Electron Microsc. Soc. 29 (1), 662–670.

Jones, B., Renaut, R., 1996. Morphology and growth of aragonite crystals in hot-spring travertines at Lake Bogoria, Kenya Rift Valley. Sedimentology 43 (2), 323–340.

Keshavarz, Z., Barnett, M.R., 2006. EBSD analysis of deformation modes in Mg–3Al–1Zn. Scr. Mater. 55 (10), 915–918.

Li, R., 1994. Characters of forms and surface microstructure of calcite crystals occurred in polymetallic deposits in South Hunan. Hunan Geol. 13 (1), 25–28.

Li, R., Dong, S., Ding, L., Shi, W., 2013. Tectonically driven organic fluid flow in Dabashan foreland belt: recorded by fibrous calcite veins contained hydrocarbon bearing inclusions. Acta Sedimentol. Sin. 31 (3), 516–526.

Liu, J., Cao, S., Zou, Y., Song, Z., 2008. EBSD analysis of rock fabrics and its application. Geol. Bull. China 27 (10), 1638–1645.

Lloyd, G., 2000. Grain boundary contact effects during faulting of quartzite: an SEM/EBSD analysis. J. Struct. Geol. 22 (11–12), 1675–1693.

Loucks, R., Reed, R., Ruppel, S., Hammes, U., 2012. Spectrum of pore types and networks in mudrocks and a descriptive classification for matrix-related mudrock pores. AAPG (Am. Assoc. Pet. Geol.) Bull. 96 (6), 1071–1098.

Luan, G., Dong, C., Azmy, K., Lin, C., Ma, C., Ren, L., Zhu, Z., 2019. Origin of bedding-parallel fibrous calcite veins in lacustrine black shale: A case study from Dongying Depression, Bohai Bay Basin. Mar. Pet. Geol. 102, 873–885.

Luo, Y., Zhao, Y., Chen, H., Su, H., 2015. Fracture characteristics under the coupling effect of tectonic stress and fluid pressure: a case study of the fractured shale oil reservoir in Liutun subsag, Dongpu Sag, Bohai Bay Basin, Eastern China. Pet. Explor. Dev. 42 (2), 177–185.

Ma, C., Dong, C., Luan, G., Lin, C., Liu, X., Elsworth, D., 2016. Types, characteristics and effects of natural fluid pressure fractures in shale: a case study of the Paleogene strata in Eastern China. Pet. Explor. Dev. 43 (4), 580–589.

Maher, H.D., Ogata, K., Braathen, A., 2017. Cone-in-cone and beef mineralization associated with Triassic growth basin faulting and shallow shale diagenesis, Edgeøya, Svalbard. Geol. Mag. 154 (2), 201–216.

Mainprice, D., Bascou, J., Cordier, P., Tommasi, A., 2004. Crystal preferred orientations of garnet: comparison between numerical simulations and electron back-scattered diffraction (EBSD) measurements in naturally deformed eclogites. J. Struct. Geol. 26 (11), 2089–2102.

Maurice, C., Quey, R., Fortunier, R., Driver, J., 2013. High angular resolution EBSD and its materials applications. Microstruct. Des. Adv. Eng. Mater. 339–365.

Meng, Q., Hooker, J., Cartwright, J., 2017. Early overpressurising in organic-rich shales during burial: evidence from fibrous calcite veins in the Lower Jurassic Shales-with-Beef Member in the Wessex Basin, UK. J. Geol. Soc. 174 (5), 869–882.

Michael, J., Schischka, J., Altmann, F., 2003. HKL Technology EBSD Application Catalogue. HKL Technology, Hobro, Denmark.

Milliken, K., Day-Stirrat, R., 2013. Cementation in mudrocks: brief review with examples from cratonic basinmudrocks. In: Chatellier, J.-Y., Jarvie, D.M. (Eds.), Critical Assessment of Shale Resource Plays: AAPG Memoir103, pp. 133–160.

Ming, X., Liu, L., Yu, M., Bai, H., Yu, L., Peng, X., Yang, T., 2016. Bleached mudstone, iron concretions, and calcite veins: a natural analogue for the effects of reducing CO_2-bearing fluids on migration and mineralization of iron, sealing properties, and composition of mudstone cap rocks. Geofluids 16 (5), 1017–1042.

Nowell, M., Wright, S., 2005. Phase differentiation via combined EBSD and XEDS. J. Microsc. 213, 296–305.

Prior, D., Boyle, A., Lan, P., Brenker, F., Cheadle, M., Day, A., Lopez, G., Peruzzo, L., Potts,

G., Reddy, S., Spiess, R., Timms, N., Trimby, P., Wheeler, J., Zetterstorm, L., 1999. The application of electron backscatter diffraction and orientation contrast imaging in the SEM to textural problems in rocks. Am. Mineral. 84, 1741–1759.
Putnis, A., Prieto, M., Fernandez-Diaz, L., 1995. Fluid supersaturation and crystallization in porous media. Geol. Mag. 132 (1), 1–13.
Qian, Y., Chen, Q., Chen, Y., Luo, Y., 2009. Mineralogical and geochemical identification for diagenetic settings of paleo-caves and fractures-filling and vugs calcites in carbonate: taking Wells S79 and S85 for example. Acta Sedimentol. Sin. 27 (6), 1027–1032.
Ramsay, J., 1980. The crack-seal mechanism of rock deformation. Nature 284, 135–139.
Shovkun, I., Espinoza, D., 2018. Geomechanical implications of dissolution of mineralized natural fractures in shale formations. J. Pet. Sci. Eng. 160, 555–564.
Taber, S., 1916. The growth of crystals under external pressure. Am. J. Sci. 41, 532–556.
Taber, S., 1918. The origin of veinlets in the Silurian and Devonian strata of central New York. J. Geol. 26 (1), 56–73.
Toy, V., Prior, D., Norris, R., 2008. Quartz fabrics in the Alpine Fault mylonites: influence of pre-existing preferred orientations on fabric development during progressive uplift. J. Struct. Geol. 30, 602–621.
Ukar, E., Lopez, R., Gale, J., Laubach, E., Manceda, R., 2017. New type of kinematic indicator in bed-parallel veins, late Jurassic–early Cretaceous Vaca Muerta formation, Argentina: EW shortening during late Cretaceous vein opening. J. Struct. Geol. 104, 31–47.
Villert, S., Maurice, C., Wyon, C., Fortunier, R., 2009. Accuracy assessment of elastic strain measurement by EBSD. J. Microsc. 233 (2), 290–301.
Wang, W., 1983. A brief discussion on the morphology of mineral crystals. Geol. Sci. Technol. Inf. 4, 5–13.
Wang, G., Ren, Y., Zhong, J., Ma, Z., Jiang, Z., 2005. Genetic analysis on lamellar calcite veins in Paleogene black shale of the Jiyang Depression. Acta Geol. Sin. 79 (6), 834–838.
Wang, M., Chen, Y., Song, G., Steele-MacInnis, M., Liu, Q., Wang, X., Zhang, X., Zhao, Z., Liu, W., Zhang, H., Zhou, Z., 2018. Formation of bedding-parallel, fibrous calcite veins in laminated source rocks of the Eocene Dongying Depression: a growth model based on petrographic observations. Int. J. Coal Geol. 200, 18–35.
Wilkinson, A., Meaden, G., Dingley, D., 2009. Mapping strains at the nanoscale using electron back scatter diffraction. Superlattice Microstruct. 45, 285–294.
Xu, Z., Wang, Q., Liang, F., Chen, F., Xu, C., 2009. Electron backscatter diffraction (EBSD) technique and its Application to study of continental dynamics. Acta Petrol. Sin. 25 (7), 1727–1736.
Yang, P., 2008. EBSD technique, geometric crystallography and materials science. J. Chin. Electron Microsc. Soc. 27 (6), 425–431.
Zaefferer, S., Wright, L., 2007. 3D characterization of crystallographic orientation in polycrystals via EBSD. Chin. J. Stereol. Image Anal. 12, 233–238.
Zhang, B., Yin, C., Gu, Z., Zhang, J., Yan, S., Wang, Y., 2015. New indicators from bedding-parallel beef veins for the fault valve mechanism. Sci. China Earth Sci. 58 (8), 1320–1336.
Zhang, J., Jiang, Z., Jiang, X., Wang, S., Liang, C., Wu, M., 2016. Oil generation induces sparry calcite formation in lacustrine mudrock, Eocene of east China. Mar. Pet. Geol. 71, 344–359.